

## Effect of electric field inhomogeneity on kinetic Alfvén wave in an inhomogeneous magnetosphere

A K Dwivedi<sup>a\*</sup> & M S Tiwari<sup>b</sup>

<sup>a</sup>Department of Physics, Harish Chandra P G College, Varanasi 221 001, India

<sup>b</sup>Department of Physics, Dr H S Gour University, Sagar 470 003, India

Received 27 October 2016; revised 23 February 2017; accepted 15 March 2017

The effect of electric field in-homogeneity perpendicular to the ambient magnetic field on Kinetic Alfvén waves in the presence of ion and electron beam velocities are investigated. In the present study we have adopted the particle aspect approach to investigate the trajectories of charged particles in the electromagnetic field of a kinetic Alfvén wave. Expressions are derived for the field-aligned current, the perpendicular current and the dispersion relation. Energy conservation method was used to obtain the growth/damping rate of the wave. The effect of inhomogeneity of electric field and electron and ion beam velocities are discussed. In present study, we assumed that the plasma is an anisotropic and with low- $\beta$ . The results are discussed for the space plasma parameter appropriate to the auroral acceleration region of the earth's magnetosphere.

**Keywords:** Kinetic Alfvén wave, Electric field in-homogeneity, Ion and electron beam, Auroral currents

### 1 Introduction

Observations from spacecraft crossing the auroral acceleration region have revealed in great detail the microphysics of particle acceleration and the variety of plasma effects that occur within this region of space<sup>1</sup>. Onishchenko *et al.*<sup>2</sup> have stated that, the spacecraft observations<sup>3-6</sup> provide the evidence that small-and large-amplitude perturbations of the drift wave and kinetic Alfvén wave (KAW) are permanently present in the near Earth's plasma environment. KAW play an important role in energy transport in driving field-aligned currents, particle acceleration and heating, inverted-V structures in auroral acceleration region, solar flares and the solar wind<sup>7-11</sup>. Additional support for KAWs role in auroral phenomena comes from global distribution maps at both low (FAST satellite) and high (Polar satellite) altitudes showing that kinetic Alfvén waves occur on auroral field lines along the entire auroral oval<sup>12-16</sup>.

The Cluster observations on 18 March 2002 in the vicinity of a reconnection X-line of the Earth's magnetopause<sup>4</sup> reveal small amplitude electromagnetic wave perturbations that have been identified as kinetic Alfvén and drift-Alfvén waves with perpendicular wavelengths of the order of the ion Larmor radius<sup>17</sup>.

Field-aligned currents are of great importance in magnetosphere-ionosphere coupling<sup>18,19</sup>. Field aligned currents play a fundamental role in the transfer of momentum along the field. They are perhaps of most importance in magnetospheric physics in the study of coupling between regions, where different dynamical conditions prevail but which are threaded by the same field<sup>20</sup>.

Observations of electric fields in the ionosphere and the magnetosphere using various techniques have led to important advances in the understanding of magnetosphere-ionosphere coupling. Electric fields of the order of hundreds of milli volts per meter have been predicted in the high latitude ionosphere, the auroral zone, magnetotail and the plasma sheet<sup>21-26</sup>. In a variety of situations in a particular at the time of substorm onset – the interplanetary magnetic field reverses its direction, and two oppositely directed inhomogeneous electric fields are reported in the plasma sheet and in the auroral zone<sup>21,22</sup>. Over the last decade it has been established that auroral luminosity is due to the impact of an accelerated electron beam coming towards the ionosphere and at the same event the upcoming ion beam has also been observed towards the magnetotail<sup>27,28</sup>. Several papers<sup>29-31</sup> considered the parallel electric field of the kinetic Alfvén waves with the magnetic mirror effects are taken into account.

\*Corresponding author (E-mail: [akdwiv@yahoo.co.in](mailto:akdwiv@yahoo.co.in))

Chen *et al.*<sup>32</sup> presented a theory of the kinetic Alfvén wave instability in presence of the field-aligned currents. Klimushkin and Mager<sup>33</sup> considered the parallel electric field of the Alfvén waves when the coupling with the compressional mode is taken into account. In the recent past particle aspect analysis was used to explain the auroral particle acceleration in the terms of Alfvén waves and kinetic Alfvén waves propagating parallel to or obliquely with respect to the ambient magnetic field<sup>26,34-37</sup>.

The main aim of this study is to investigate the effect of ion and electron beams on the kinetic Alfvén wave in the presence of an inhomogeneous electric field in the auroral region by using particle aspect analysis. The theory is based on Dawson's theory of Landau damping which was further extended by many researchers<sup>26,35-41</sup> for the analysis of electrostatic and electromagnetic waves. The advantage of this approach is its suitability for dealing with auroral electrodynamics and energy exchange by wave-particle resonant interaction.

## 2 Basic Assumptions

In this model, the plasma is divided into two groups of particles: resonant and non-resonant. It is supposed that resonant electrons participate in the energy exchange with waves, whereas non-resonant particles support the oscillatory nature of the waves. A wave propagating obliquely to the magnetic field in a plane normal to the density gradient and applied electric field is considered, in an anisotropic plasma. The ambient magnetic field is directed along the  $z$ -axis, and the density gradient and perpendicular electric field are in the  $y$ -direction. The wave is propagating in the  $(x, z)$  plane. We have taken density gradient and related drift velocity in our analysis. The effect of pressure gradient and related current is ignored as the approximation suitable to the auroral acceleration region.

The kinetic Alfvén wave is assumed to originate at  $t = 0$  when the resonant particles are undisturbed. We consider low  $\beta$  (ratio of plasma pressure to the magnetic pressure) collision less plasma satisfying the conditions.

$$V_{T\parallel i} \ll \frac{\omega}{k_{\parallel}} \ll V_{T\parallel e}; \omega \ll \Omega_i, \Omega_e; k_{\perp}^2 \rho_e^2 \ll k_{\perp}^2 \rho_i^2 < 1 \dots (1)$$

Where  $V_{T\parallel i}$  and  $V_{T\parallel e}$  are the thermal velocities of ions and electrons along the magnetic field,  $\Omega_{i,e}$  are

gyration frequencies and  $\rho_{i,e}$  the mean gyroradii of the respective species.

We consider a kinetic Alfvén wave of the form<sup>26,34-37</sup>.

$$E = E_{\perp} + E_{\parallel} \quad \dots (2)$$

Where

$$E_{\perp} = -\nabla_{\perp} \phi, \quad E_{\parallel} = -\nabla_{\parallel} \psi$$

and

$$\phi = \phi_1 \cos(k_{\perp} x + k_{\parallel} z - \omega t), \quad \dots (3a)$$

$$\psi = \psi_1 \cos(k_{\perp} x + k_{\parallel} z - \omega t) \quad \dots (3b)$$

Where  $\phi_1$  and  $\psi_1$  are assumed to be a slowly varying function of time  $t$ , and  $\omega$  is the wave frequency.  $k_{\perp}$  and  $k_{\parallel}$  define the components of wave vector  $\underline{k}$  perpendicular and parallel to the magnetic field  $B_0$ . Electrons streaming with their thermal velocity along the field lines are assumed to interact with the electric field of the kinetic Alfvén wave. Electrons whose velocity is slightly less than the parallel phase velocity  $\omega/k_{\parallel}$  of the wave cause Landau damping of the wave. The inhomogeneous applied electric field  $E_{(y)}$  has the form of a stable mode, and is given as<sup>26</sup>:

$$E_{(y)} = E_0 \left( 1 - \frac{y^2}{a^2} \right)$$

Where  $a$  is taken to be comparable to the mean ion gyroradius but much larger than the Debye length. The model related to the electric field representation may be pertaining to the two oppositely directed electric fields in the auroral acceleration region.  $y = 0$  represents maximum electric field at the mid-plane of the acceleration region which decreases both the sides of the central part by increasing the value of  $y$  and attains zero value at  $y = a$  of the order of the ion gyroradius. The variations as the square of  $y$  coordinate predicts two oppositely directed electric fields similar in nature. When  $y^2/a^2 \ll 1$ ,  $E_{(y)}$  becomes a constant uniform field. In the case  $y > a$ , the electric field changes sign and is oppositely directed.

## 3 Distribution Function

We adopt the perturbed density for non-resonant particles in the presence of the kinetic Alfvén wave

for the inhomogeneous plasma<sup>26</sup>. To determine the dispersion relation and the associated currents, we use the distribution function of the form<sup>37</sup>

Where

$$f_{\perp}(V_{\perp}) = \frac{m}{2\pi T_{\perp}} \exp\{-mV_{\perp}^2/2T_{\perp}\} \dots (5)$$

$$f_{\parallel}(V_{\parallel}) = \left(\frac{m}{2\pi T_{\parallel}}\right)^{1/2} \exp\left\{-m(V_{\parallel} - V_{Dj})^2 / 2T_{\parallel}\right\} \dots (6)$$

Where  $\varepsilon$  is a small-scale parameter of the order of inverse of the density gradient scale length.  $V_{Dj}$  defines the beam velocity of the particles. Here  $m$  is the mass and,  $T_{\perp}$  &  $T_{\parallel}$  are the temperatures of charged particles perpendicular and parallel to the magnetic field  $B_0$  which is directed along the z-axis. The wave is propagating in x-z plane normal to density gradient which is along the y-axis.

#### 4 Dispersion Relation

The integrated perturbed density for non-resonant particles  $n_{i,e}$  is given as

$$n_{i,e} = \int_0^{\infty} 2\pi V_{\perp} dV_{\perp} \int_{-\infty}^{\infty} dV_{\parallel} n_1(r, t) \dots (7)$$

We use the expression of  $n_1$  for non-resonant particles which has been evaluated by Baronia and Tiwari<sup>26</sup> as

$$n_1(r, t) = N(V) \sum_{-\infty}^{\infty} J_n(\mu) \sum_{-\infty}^{\infty} J_l(\mu) \frac{q}{m} \left[ \left\{ \phi_1 - \frac{V_{\parallel} k_{\parallel}}{\omega} (\phi_1 - \psi_1) \right\} \times \left\{ \frac{k_{\perp}^2}{a_n^2} - \frac{\Omega^2 V_d^i k_{\perp} m}{\Lambda_n a_n^2 T_{\perp}} \right\} + \frac{k_{\parallel}^2}{\Lambda_n^2} \psi_1 \right] \cos \xi_{nl} \dots (8)$$

$V_d^i$  is the diamagnetic drift velocity which is defined by

$$V_d^i = \frac{T_{\perp}}{m\Omega} \frac{1}{N} \frac{\partial N}{\partial y} \dots (9)$$

and  $V_d^i = 0$ , represents the homogeneous plasma,  $q$  is the charge which is equal to  $e$  for ions and  $-e$  for electrons.

$$\mu = \frac{k_{\perp} V_{\perp}}{\Omega} \left[ 1 + \frac{3}{4} \frac{E'_{\perp}(y)}{\Omega^2} \right],$$

$$\Lambda_n = k_{\parallel} V_{\parallel} - \omega + n\Omega + k_{\perp} \tilde{\Delta}$$

$$\tilde{\Delta} = -\frac{\bar{E}(y)}{\Omega} \left[ 1 + \frac{E''(y)}{E(y)} \frac{1}{4} \left( \frac{V_{\perp}}{\Omega} \right)^2 + \dots \dots \dots \right]$$

where

$$\bar{E}(y) = \frac{q}{m} E(y)$$

$$a_n^2 = \Lambda_n^2 - \Omega^2,$$

$$\xi_{nl} = k_{\perp} y + k_{\parallel} z - \omega t + (n-l)(\Omega t - \theta) \dots (10)$$

$\theta$  is the initial phase of the charges particles,  $n$  and  $l$  are running symbols and integer. In view of the approximations (Eq. 3), the dominant contribution comes from the term  $n = l = 0$  as the contributions due to higher  $n$  are negligible<sup>39</sup>. The resonant criterion is

given by  $k_{\parallel} V_{\parallel} - \omega + k_{\perp} \tilde{\Delta} = 0$ , which means that the electrons see the wave independent of  $t$  in the

particles frame. Here  $\tilde{\Delta}$  represents  $E \times B$  drift velocity of the particles modified by the inhomogeneity of the electric field. In definition of the resonant criteria we have ignored the effect of inhomogeneity of electric field due to large scale length of the inhomogeneity, otherwise would lead drift instability by feedback mechanism<sup>42</sup>. The particles satisfying the above condition are called resonant.  $J_s$  are Bessel's functions which arise from the different periodical variation of charged particles trajectories. The term represented by Bessel's functions show the reduction of the field intensities due to finite gyroradius effect. With the help of Eqs (4) and (8) we find the average densities for inhomogeneous plasma

$$\bar{n}_i = \frac{\omega_{pi}^2}{4\pi e} \left[ -\frac{k_{\perp}^2 \phi}{\Omega^2} + \frac{k_{\parallel}^2 \psi}{\omega_i^2} + \frac{k_{\perp} V_d^i m_i}{\omega_i T_{\perp i}} \right] \left( 1 - \frac{1}{2} k_{\perp}^2 \rho_i^2 \right) \dots (11)$$

$$\bar{n}_e = \frac{\omega_{pe}^2}{4\pi e V_{T\parallel e}^2} \psi$$

$$\omega_{pi,e}^2 = 4\pi N_0 e^2 / m_{i,e} \dots (12)$$

Where  $V_{T\parallel e}^2$  is the square of thermal velocity parallel to the ambient magnetic field.  $V_d^i$  is the diamagnetic drift velocity of ions. Using the quasi-neutrality condition<sup>7,26,36,37</sup>

$$\bar{n}_i = \bar{n}_e, \quad \dots (13)$$

We get the relation between  $\phi$  and  $\psi$  as

$$\frac{\phi}{\psi} = -\frac{\Omega_i^2}{k_\perp^2} \left[ \frac{\omega_{pe}^2}{\omega_{pi}^2 V_{T\parallel e}^2 \left(1 - \frac{1}{2} k_\perp^2 \rho_i^2\right)} - \frac{k_\parallel^2}{\omega_i^2} \right] D_d \dots (14)$$

Using perturbed ion and electron densities  $n_i$  and  $n_e$  and Amperes law in parallel direction<sup>7,36,37</sup>, we obtain the relation

$$\frac{\partial}{\partial z} \nabla_\perp^2 (\phi - \psi) = \frac{4\pi}{c^2} \frac{\partial}{\partial t} J_Z, \quad \dots (15)$$

where

$$J_Z = e \int_0^\infty 2\pi V_\perp dV_\perp \int_{-\infty}^\infty dV_\parallel [(N(V)u_z(r,t) + V_\parallel p_1(r,t))_i - (N(V)u_z(r,t) + V_\parallel p_1(r,t))_e] \quad \dots (16)$$

$u_z(r,t)$  is the perturbed velocity of charged particles in the presence of a kinetic Alfvén wave.  $J_Z$  is the current density which involves first-order perturbations of density and velocity. The expression for  $u_z(r,t)$  is calculated by Baronia and Tiwari<sup>26</sup>, which is given as

$$u_z(r,t) = -\frac{q}{m} \left[ \psi_1 k_\parallel + \frac{V_\perp k_\parallel k_\perp}{\omega} (\phi_1 - \psi_1) \frac{n}{\mu} \right] \sum_{-\infty}^\infty J_n(\mu) \sum_{-\infty}^\infty J_l(\mu) \times \frac{1}{\Lambda_n} [\cos \xi_{nl} - \eta \cos(\xi_{nl} - \Lambda_n t)], \quad \dots (17)$$

Where  $\eta = 0$  for the non-resonant particles and  $\eta = 1$  for the resonant one. In the analysis we have assumed the plasma consisting of non-resonant and resonant particles. The non-resonant particles support the oscillatory motion of the wave, whereas the resonant particles participate in energy exchange with the wave. To distinguish the non-resonant and resonant particles we have adopted the symbol  $\eta = 0$  for non-resonant particles and  $\eta = 1$  for the resonant particles<sup>37</sup>. The methodology of this paper is based upon the particle aspect analysis<sup>37</sup> which is focused to

evaluate the particle trajectories in the presence of wave electromagnetic fields.

With the help of Eqs (14) and (15) we obtain the dispersion relation for the kinetic Alfvén wave in inhomogeneous plasma as:

$$\begin{aligned} & \left( 1 - \frac{\omega_i^2}{k_\parallel^2 c_s^2 A} \right) \left( 1 - \frac{\omega^2 A}{k_\parallel^2 v_A^2} D_d \right) + \frac{(\omega - k_\parallel V_{De}) \omega_i E^A}{k_\parallel^2 v_A^2} D_d \\ & = \frac{k_\perp^2 \omega^2}{k_\parallel^2 \Omega_i^2} D_d - \left( \frac{\omega_{pe}^2}{\omega_{pi}^2 V_{T\parallel e}^2 A} - \frac{k_\parallel^2}{\omega_i^2} \right) \\ & \times A \left( \frac{\omega_{pi}^2 \omega_i^2 T_{\parallel i}}{c^2 \Omega_i^2 k_\parallel^2 m_i} - \frac{V_d^i k_\perp m_i \omega_{pi}^2 \omega_i^2 A}{T_{\perp i} c^2 k_\parallel^3 k_\perp^2} \right) \end{aligned} \quad \dots (18)$$

Where

is the square of ion-acoustic speed and

$$v_A^2 = \frac{c^2 \Omega_i^2}{\omega_{pi}^2}$$

is the square of Alfvén speed. The dispersion relation of the kinetic Alfvén wave reduces to that derived by Hasegawa and Chen<sup>41</sup>, Baronia and Tiwari<sup>26</sup> under the approximation,  $V_d^i = 0$ ,  $V_{Di} = 0$ ,  $V_{De} = 0$  and  $I_0(\lambda_i) \exp(-\lambda_i) \sim 1 - \lambda_i$ , for  $\lambda_i = \frac{1}{2} k_\perp^2 \rho_i^2 < 1$  as we have applied.  $I_0(\lambda_i)$  is the modified Bessel function.

## 5 Current Density

Since the average value of current vanishes which is contributed by first-order perturbations of density and velocity due to their periodical variations, we evaluate the average current per unit wavelength which is the second-order perturbation. To evaluate the perturbed current density per unit wavelength we use the following set of equations

$$\bar{J}_{i,e} = \int_0^\lambda ds \int_0^\infty 2\pi V_\perp dV_\perp \int_{-\infty}^\infty dV_\parallel e^{i(N+n_1)(\bar{v} + \bar{u}) - N\bar{v}} \quad \dots (19)$$

$$\text{And } \bar{J} = \bar{J} - \bar{J}_e \quad \dots (20)$$

With the help of Eqs (4), (8) and (17) we obtain following relations:

$$J_X = \frac{\psi_1 e k_{\perp} k_{\parallel}^2 \lambda}{8\pi} \left[ \frac{\omega_{pe}^2}{m_e \Omega_e^2} \left\{ \left( \frac{\phi_1 - \psi_1}{\omega} \right) \left( 1 - \frac{2\omega_e^2}{k_{\parallel}^2 V_{T\parallel e}^2} \right) + \frac{2\omega_e}{k_{\parallel}^2 V_{T\parallel e}^2} \phi_1 \right\} - \frac{\omega_{pi}^2 (1 - k_{\perp}^2 \rho_i^2) \phi_1}{m_i \Omega_i^2 \omega_i} \right] \dots (21)$$

$$J_Z = \frac{e \psi_1 k_{\parallel} \lambda}{8\pi} \left[ \frac{\omega_{pe}^2}{m_e} \left\{ \frac{k_{\perp}^2}{\Omega_e^2} \left( \frac{\phi_1 - \psi_1}{\omega} \right) + \frac{2\omega_e \psi_1}{k_{\parallel}^2 V_{T\parallel e}^2} \right\} - \frac{8\omega_e}{k_{\parallel}^2 V_{T\parallel e}^4} \psi_1 \right] - \frac{\omega_{pi}^2}{m_i} \left\{ \frac{k_{\perp}^2}{\Omega_i^2 \omega_i} \phi_1 - \frac{4\psi_1}{k_{\parallel}^2 V_{T\parallel i}^2} + \frac{4\psi_1}{V_{T\parallel i}^2 \omega_i} \right\} \left( 1 - k_{\perp}^2 \rho_i^2 \right) \dots (22)$$

Where

$$\omega_e = \omega - \omega_i E - k_{\parallel} |VDe$$

In the evaluation of the current densities it was assumed that the field-aligned and perpendicular currents are due to an electromagnetic kinetic Alfvén wave and the contribution due to diamagnetic drift was neglected.

## 6 Growth/Damping Rate

Evaluating the wave energy density per unit wavelength and changes in energy of non-resonant and resonant particles, Terashima<sup>38</sup>, Varma and Tiwari<sup>40</sup> and Dwivedi *et al.*,<sup>36,37</sup> have derived the growth/damping rate by performing a considerable amount of algebraic calculations, which is of the form

$$\gamma = (1/\psi_1)(d\psi_1/dt)$$

$$\gamma = A\omega(T_{\parallel e}/m_e) \left\{ \frac{k_{\perp} V_d^e}{k_{\parallel}(T_{\parallel e}/m_e)} f_{\parallel e}(\omega/k_{\parallel}) + f'_{\parallel e}(\omega/k_{\parallel})^3 \right\} \dots (23)$$

Substituting Eq. (6) we finally obtain the growth/damping-rate as

$$\gamma/\omega = \pi^{1/2} \frac{\omega_e^2}{\omega k_{\parallel} |V_{T\parallel e}|} \left( \frac{T_{\parallel e} k_{\perp} V_d^e}{T_{\perp e} \omega_e} - 1 \right) \exp \left[ -\frac{\omega_e^2}{k_{\parallel}^2 V_{T\parallel e}^2} \right] \dots (24)$$

Where  $V_{T\perp\parallel}^2 = (2T_{\perp\parallel}/m)$ ;  $V_d^e$  represents electron diamagnetic drift velocity and the value of  $\omega$  for the drift kinetic Alfvén wave has to be submitted. In case of  $V_{De} = 0$  we recover the growth rate as derived by Dwivedi *et al.*<sup>36,37</sup>, Baronia and

Tiwari<sup>26,34</sup>. The kinetic Alfvén waves are generated by density inhomogeneity if the electric field inhomogeneity is absent. However, due to the electric field inhomogeneity the condition is altered.

The electric field inhomogeneity required for wave excitation can be estimated by the marginally stable condition ( $\gamma = 0$ ), under the approximation  $\omega/k_{\parallel} V_{T\parallel e} < 1$ , we obtain

$$\delta \approx 1 - \frac{B_0}{k_{\perp} E_0} \left( \omega - k_{\parallel} |VDe - \frac{T_{\parallel e}}{T_{\perp e}} k_{\perp} V_d^e \right) \dots (25)$$

Which is of the order of 0.89 for  $k_{\perp} \rho_i = 0.5$ ,  $\omega = 6.2 \times 10^3 \text{ s}^{-1}$ ,  $V_{De} = 1 \times 10^7 \text{ cm/s}$ ,

$V_{Di} = -4 \times 10^5 \text{ cm/s}$ ,  $E_0 = 50 \text{ mV m}^{-1}$ , and the parameters used in result and discussion

## 7 Result and Discussion

In the numerical evaluation of the growth-rate, current and dispersion, we have used the following parameters for the auroral acceleration region<sup>26,27,34-37</sup>

$B_0 = 4300 \text{ nT}$ ,  $\Omega_i = 412 \text{ s}^{-1}$ ,  $KT_{\parallel i} = 1 \text{ keV}$ ,  $KT_{\parallel e} = 10 \text{ keV}$ ,  $V_d^e = 200 \text{ cm/s}$ ,  $\omega_{pi}/\Omega_i = 10$  and  $K$  is the Boltzmann constant.

### 7.1 Dispersion relation

The dispersion relation Eq. (18) has been solved numerically using the Newton-Raphson method and the value of  $\omega$  are plotted versus  $k_{\perp} \rho_i$  in Fig. 1. It is clear that the wave frequency  $\omega$  increases with

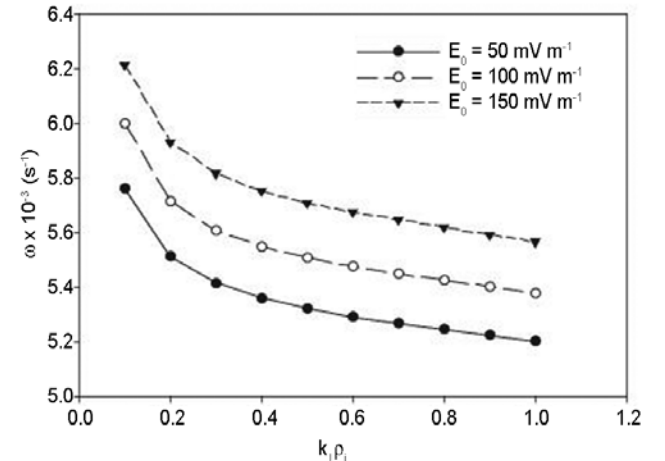


Fig. 1 — Frequency ( $\omega$ ) versus perpendicular wave number ( $k_{\perp} \rho_i$ ) for different  $E_0$ ;  $V_{Di} = -4 \times 10^5 \text{ cm/s}$ ;  $V_{De} = 1 \times 10^7 \text{ cm/s}$ ;  $\delta = 0.4$

increase of the applied electric field. The decrease of  $\omega$  with increasing  $k_{\perp}\rho_i$  is due to the finite Larmor-radius effect. The effect of electric field inhomogeneity on wave frequency is depicted in Fig. 2. The wave frequency decreases with increasing degree of inhomogeneity. Wave frequency decreases

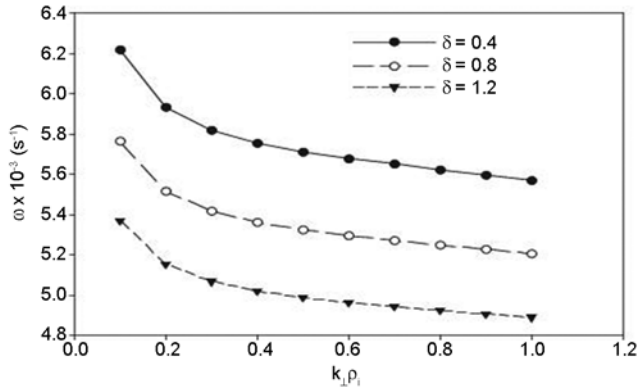


Fig. 2 — Frequency ( $\omega$ ) versus perpendicular wave number ( $k_{\perp}\rho_i$ ) for different  $\delta$ ;  $V_{Di} = -4 \times 10^5$  cm/s;  $V_{De} = 1 \times 10^7$  cm/s;  $E_0 = 150$  mV m $^{-1}$

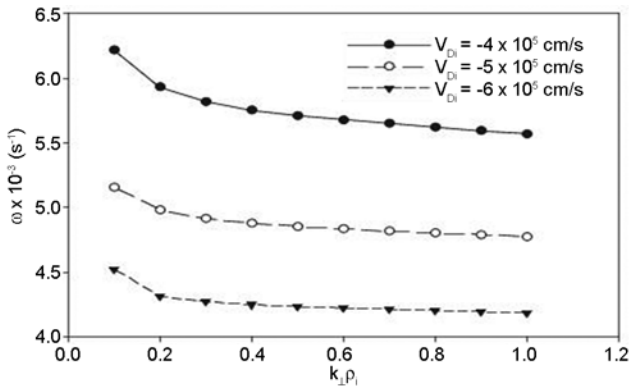


Fig. 3 — Frequency ( $\omega$ ) versus perpendicular wave number ( $k_{\perp}\rho_i$ ) for different ion beam velocity  $V_{Di}$ ;  $V_{De} = 1 \times 10^7$  cm/s;  $E_0 = 150$  mV m $^{-1}$ ;  $\delta = 0.4$

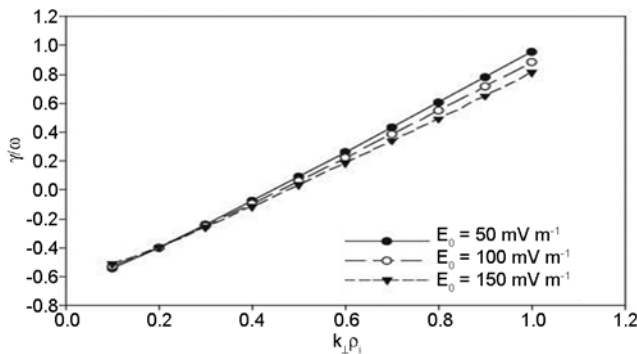


Fig. 4 — Growth/damping rate ( $\gamma/\omega$ ) versus perpendicular wave number ( $k_{\perp}\rho_i$ ) for different  $E_0$ ;  $V_{Di} = -4 \times 10^5$  cm/s;  $V_{De} = 1 \times 10^7$  cm/s;  $\delta = 0.4$

with increase of  $k_{\perp}\rho_i$ . Figure 3 shows the variation of wave frequency  $\omega$  with  $k_{\perp}\rho_i$  for different value of ion beam velocities. It is observed that wave frequency decreases with increase of ion beam velocities.

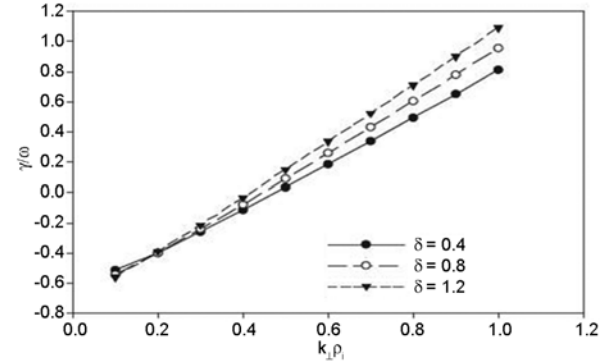


Fig. 5 — Growth/damping rate ( $\gamma/\omega$ ) versus perpendicular wave number ( $k_{\perp}\rho_i$ ) for different  $\delta$ ;  $V_{Di} = -4 \times 10^5$  cm/s;  $V_{De} = 1 \times 10^7$  cm/s;  $E_0 = 150$  mV m $^{-1}$

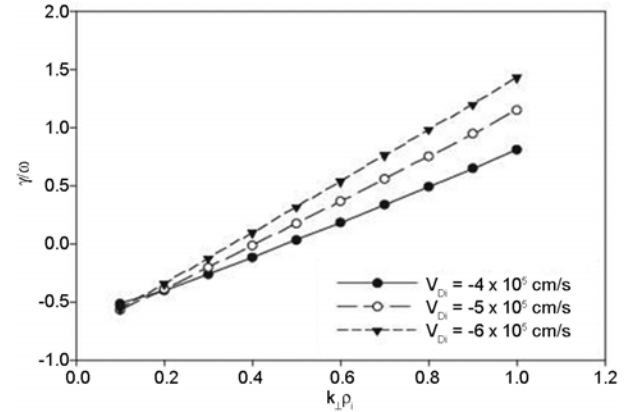


Fig. 6 — Growth/damping rate ( $\gamma/\omega$ ) versus perpendicular wave number ( $k_{\perp}\rho_i$ ) for different ion beam velocity  $V_{Di}$ ;  $V_{De} = 1 \times 10^7$  cm/s;  $E_0 = 150$  mV m $^{-1}$ ;  $\delta = 0.4$

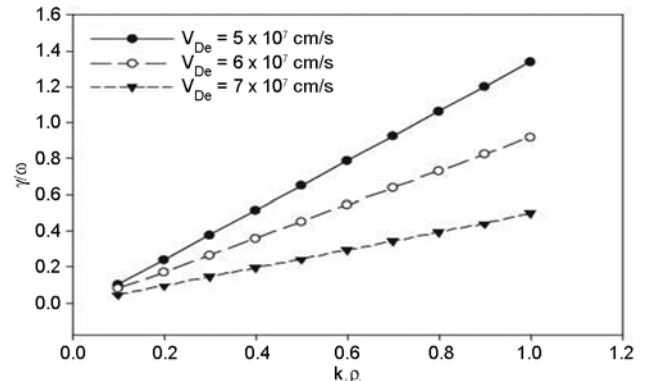


Fig. 7 — Growth/damping rate ( $\gamma/\omega$ ) versus perpendicular wave number ( $k_{\perp}\rho_i$ ) for different electron beam velocity  $V_{De}$ ;  $V_{Di} = -4 \times 10^5$  cm/s;  $E_0 = 150$  mV m $^{-1}$ ;  $\delta = 0.4$

### 7.2 Growth/damping rate

Figures 4 and 5 show the variation of growth/damping rate with  $k_{\perp}\rho_i$  for different value of electric field and electric field inhomogeneity, respectively. It is observed that electric field decreases the growth/damping rate, whereas electric field inhomogeneity increases the growth/damping rate. It is also found that wave is damped at lower  $k_{\perp}\rho_i$  while excited at higher  $k_{\perp}\rho_i$ . Electric field and electric

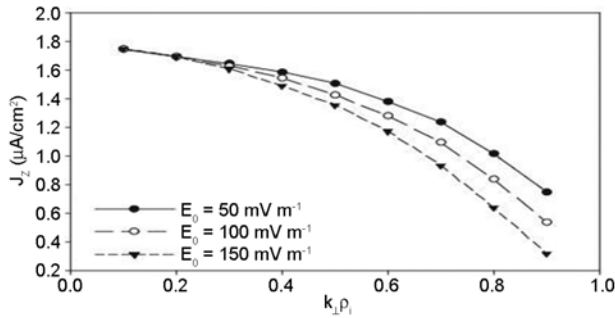


Fig. 8 — Parallel current ( $J_z$ ) versus perpendicular wave number ( $k_{\perp}\rho_i$ ) for different  $E_0$ ;  $V_{Di} = -4 \times 10^5$  cm/s;  $V_{De} = 1 \times 10^7$  cm/s;  $\delta = 0.4$

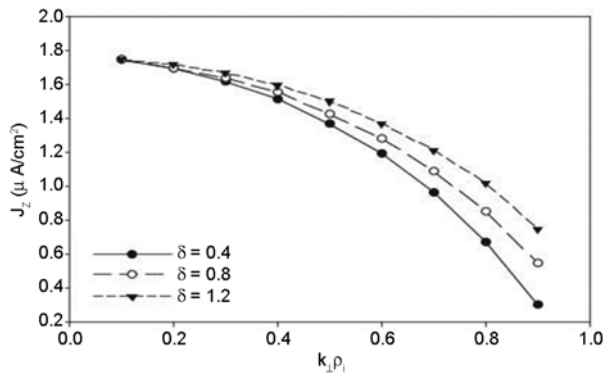


Fig. 9 — Parallel current ( $J_z$ ) versus perpendicular wave number ( $k_{\perp}\rho_i$ ) for different  $\delta$ ;  $V_{Di} = -4 \times 10^5$  cm/s;  $V_{De} = 1 \times 10^7$  cm/s;  $E_0 = 150$  mV m $^{-1}$

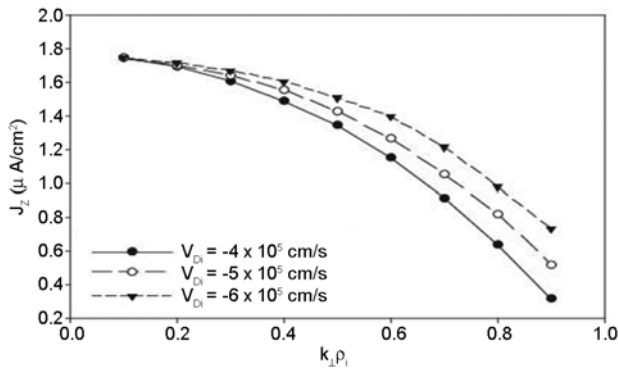


Fig. 10 — Parallel current ( $J_z$ ) versus perpendicular wave number ( $k_{\perp}\rho_i$ ) for different ion beam velocity  $V_{Di}$ ;  $V_{De} = 1 \times 10^7$  cm/s;  $E_0 = 150$  mV m $^{-1}$ ;  $\delta = 0.4$

field inhomogeneity are more effective at higher  $k_{\perp}\rho_i$ . Figures 6 and 7 show the variation of growth/damping rate with  $k_{\perp}\rho_i$  for different value of ion and electron beam velocities. The ion beam velocity enhances the

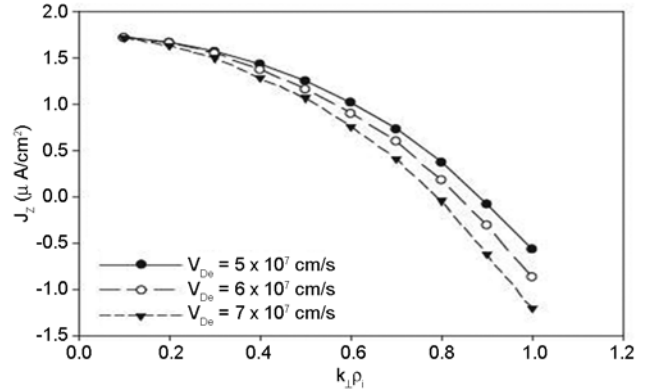


Fig. 11 — Parallel current ( $J_z$ ) versus perpendicular wave number ( $k_{\perp}\rho_i$ ) for different electron beam velocity  $V_{De}$ ;  $V_{Di} = -4 \times 10^5$  cm/s;  $E_0 = 150$  mV m $^{-1}$ ;  $\delta = 0.4$

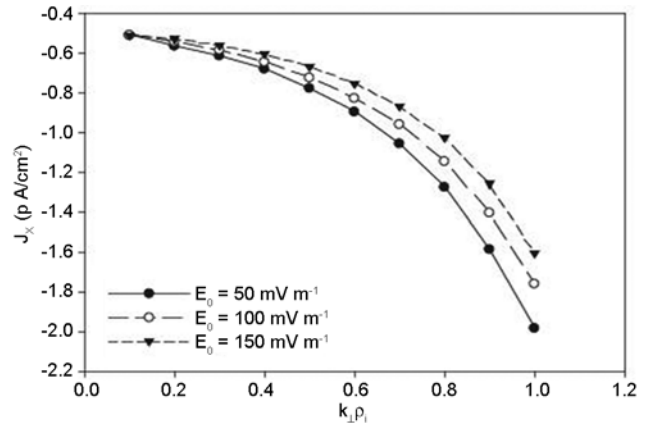


Fig. 12 — Perpendicular current ( $J_x$ ) versus perpendicular wave number ( $k_{\perp}\rho_i$ ) for different  $E_0$ ;  $V_{Di} = -4 \times 10^5$  cm/s;  $V_{De} = 1 \times 10^7$  cm/s;  $\delta = 0.4$

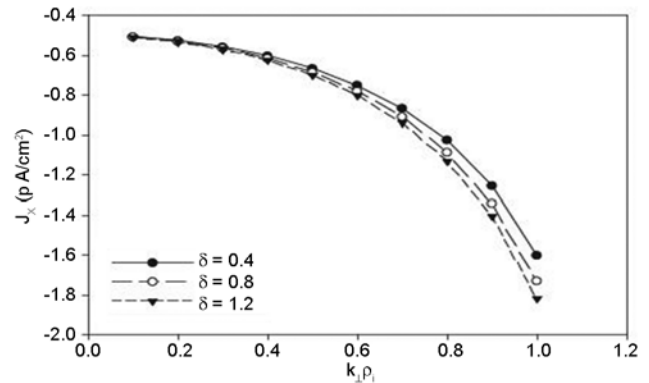


Fig. 13 — Perpendicular current ( $J_x$ ) versus perpendicular wave number ( $k_{\perp}\rho_i$ ) for different  $\delta$ ;  $V_{Di} = -4 \times 10^5$  cm/s;  $V_{De} = 1 \times 10^7$  cm/s;  $E_0 = 150$  mV m $^{-1}$

growth/damping rate whereas electron beam reduces the growth/damping rate. No damping rate is observed in the case of electron beam velocity.

### 7.3 Electric current

The effect of electric field and electric field inhomogeneity on parallel current is shown in Figs 8 and 9. The electric field decreases the parallel current whereas electric field inhomogeneity increases the parallel current. Figures 10 and 11 show the variation of parallel current with  $k_{\perp}\rho_i$  for different value of ion and electron beam velocity. It is seen that ion beam velocity increases the parallel current, while electron beam velocity decreases the parallel current. The decreasing value of  $J_z$  is seen for higher value of  $k_{\perp}\rho_i$ . Thus the magnitude of the field-aligned current may depend upon the perpendicular wave number and the ion gyroradius. Figures 12 and 13 show the variation of the perpendicular current with  $k_{\perp}\rho_i$  for different value of electric field and electric field inhomogeneity. It is observed that electric field enhance the perpendicular current whereas electric field inhomogeneity reduces the perpendicular current. The effect of ion and electron beam velocity on perpendicular current is shown in Figs 14 and 15, the ion beam velocity decreases the perpendicular current whereas electron beam velocity increases the perpendicular current, the perpendicular current also decreases with  $k_{\perp}\rho_i$ . It is also seen that ion and electron beam velocities are more effective towards higher  $k_{\perp}\rho_i$ .

## 8 Conclusions

The kinetic Alfvén wave may be generated in the distant magnetosphere either by ion and electron beam velocity or electric field inhomogeneity or density inhomogeneity<sup>20</sup> at substorm times and propagates towards the ionosphere leading to acceleration and current pattern as reported by Freja and FAST satellite data. The present investigation of kinetic Alfvén wave incorporates the effectiveness of electric field inhomogeneity in the presence of ion and electron beam. It is noticed that ion and electron beams are much effective towards higher  $k_{\perp}\rho_i$  in the presence of electric field inhomogeneity as compared to earlier work<sup>37</sup>. It is also noticed that electric field inhomogeneity is more effective on parallel current in the presence of ion and electron beam as compared to earlier work<sup>26</sup>. The electric field inhomogeneities support the kinetic Alfvén wave generation. The particle aspect analysis adopted here also to predict

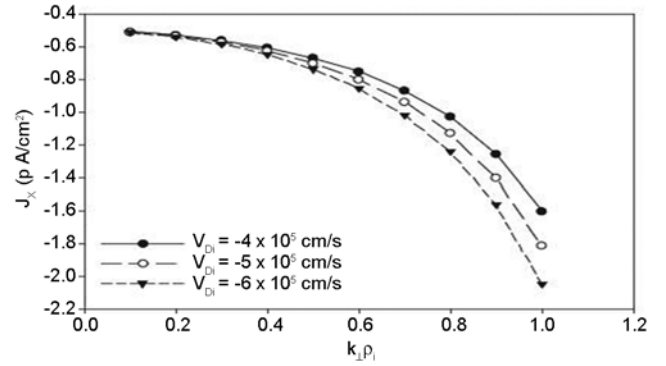


Fig. 14 — Perpendicular current ( $J_x$ ) versus perpendicular wave number ( $k_{\perp}\rho_i$ ) for different ion beam velocity  $V_{Di}$ ;  $V_{De} = 1 \times 10^7$  cm/s;  $E_0 = 150$  mV m<sup>-1</sup>;  $\delta = 0.4$

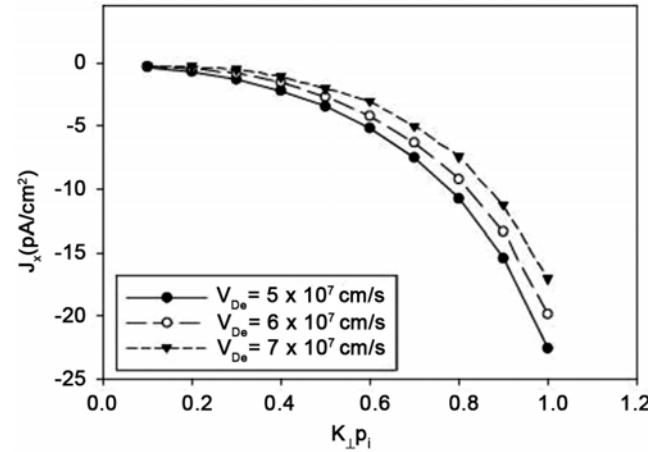


Fig. 15 — Perpendicular current ( $J_x$ ) versus perpendicular wave number ( $k_{\perp}\rho_i$ ) for different electron beam velocity  $V_{De}$ ;  $V_{Di} = -4 \times 10^5$  cm/s;  $E_0 = 150$  mV m<sup>-1</sup>;  $\delta = 0.4$

the currents associated with the wave.

The ion and electron beams are capable of generating kinetic Alfvén wave and the direction of current is controlled by the electron and ion beam velocities. In the past variety of theories are produced for the development of parallel electric fields on auroral field lines. This parallel electric field may lead upflowing ion beam and downcoming electron beam which may generate the kinetic Alfvén waves and adjust the current pattern on auroral field lines. The wave frequency, current pattern and wave numbers are also influenced by the electric field inhomogeneity, and electron and ion beam. The direction and magnitude of the current depend strongly upon the finite-gyroradius effect, which also controls the wave spectrum. The present investigation may be useful to explain observed Poynting flux<sup>43,44</sup> along auroral field lined towards the earth by the large scale Alfvénic waves. The waves generated above the



acceleration region are supported by electric field inhomogeneity in the presence of ion and electron beams carry energy towards earth's ionospheric regions to display aurora. Including the effect of electric field inhomogeneity and effect of ion and electron beam the FAST and Freja observations may be explained more reasonably.

## References

- 1 Pschmann G, Haaland S & Treumann R, *Auroral Plasma Physics*, (Kluwer Acad., Dordrecht, Netherland), 2003.
- 2 Onishchenko O G, Pokhotelov O A, Kranoselskikh V V & Shatalov S I, *Ann Geophys*, 27 (2009) 639.
- 3 Chemyrev V M, Bilichenko S V, Pokhotelov O A, Marchenko V M, Lazarev V I, Streltsov A V & Stenflo L, *Phys Scr*, 38 (1988) 841.
- 4 Chaston C C, Phan T D, Bonnell J W, Mozer F S, Accuna M, Goldstein M L, Balogh A, Andre M, Reme H & Fazakerley A, *Phys Rev Lett*, 95 (2005) 065002.
- 5 Sundkvist D, Vladimir K, Shukla P K, Vaivads A, Andre M, Buchert S & Reme H, *Nature*, 436 (2005) 825.
- 6 Sundkvist D, Vaivads A, Andre M, Wahlund J E, Hobara Y, Joko S, Krasnoselskikh V V, Bogdanova Y V, Buchert S C, Cornilleau-Wehrin N, Fazakerley A, Hall J O, Reme H & Stenberg G, *Ann Geophys*, 23 (2005) 983.
- 7 Hasegawa A, *Proc Ind Acad Sci*, 86A (1997) 151.
- 8 Goertz C K & Boswell R W, *J Geophys Res*, 84 (1979) 7293.
- 9 Goertz C K, *Planet Space Sci*, 32 (1984) 1387.
- 10 Maghaddam-Taaheri E, Goertz C K & Smith R A, *J Geophys Res*, 94 (1989) 10047.
- 11 Huang G L & Wang R Y, *J Plasma Phys*, 58 (1997) 433.
- 12 Chaston C C, *Geophys Res Lett*, 31 (2004) 3811.
- 13 Chaston C C, Carlson C W, Ergun R W, McFadden J P & Strangeway R J, *J Geophys Res*, 108 (A4) (2003) 8003.
- 14 Keiling A, Wygant J R, Cattell C, Johnson M, Temerin M, Moser F S, Kletzing C A, Scudder J & Russell C T, *J Geophys Res*, 106 (2001) 5779.
- 15 Keiling A, Wygant J R, Cattell C A, Mozer F S & Russell C T, *Science*, 299 (2003) 383.
- 16 Keiling A, Parks G K, Wygant J R, Dombeck J, Mozer F S, Russell C T, Streltsov A V & Lotko W, *J Geophys Res*, 110 (A9) (2005) 10.
- 17 Agarwal P, Varma P & Tiwari M S, *Astr Space Sci*, 345 (2013) 99.
- 18 Agarwal P, Varma P & Tiwari M S, *Planet Space Sci*, 59 (2011) 306.
- 19 Agarwal P, Varma P & Tiwari M S, *Planet Space Sci*, 71 (2012) 101.
- 20 Southwood D J & Kivelson M G, *J Geophys Res*, 96 (1991) 67.
- 21 Mozer F S & Lucht P, *J Geophys Res*, 79 (1974) 1001.
- 22 Candidi M & Orsini S, *Geophys Res Lett*, 8 (1981) 637.
- 23 Cattell C A, Mozer F S, Hones E W Jr, Anderson R R & Sharp R D, *J Geophys Res*, 91 (1986) 5663.
- 24 Mauk B H & Zenetti L J, *Rev Geophys*, 25 (1987) 541.
- 25 Providakes J F, Kelley M C & Swartz W E, *J Geophys Res*, 94 (1989) 5350.
- 26 Baronia A & Tiwari M S, *J Plasma Phys*, 63 (2000) 311.
- 27 Tiwari M S & Rostoker G, *Planet Space Sci*, 32 (1984) 1497.
- 28 Mozer F S, Wygant J R, Boehm M H, Cattell C A & Temerin M, *Space Sci Rev*, 42 (1985) 313.
- 29 Nakamura T K, *J Geophys Res*, 105 (2000) 10729.
- 30 Tikhonchuk V T & Rankin R, *J Geophys Res*, 107 (2002) SMP 11-1.
- 31 Lysak R L & Song Y, *J Geophys Res*, 110 (2005) A10S06.
- 32 Chen L, Wu D J & Huang J, *J Geophys Res*, 118 (2013) 2951.
- 33 Klimushkin D Y & Mager P N, *Astrophys Space Sci*, 350 (2014) 579.
- 34 Baronia A & Tiwari M S, *Planet Space Sci*, 47 (1999) 1111.
- 35 Dwivedi A K, Varma P & Tiwari M S, *Planet Space Sci*, 49 (2001) 993.
- 36 Dwivedi A K, Varma P & Tiwari M S, *Planet Space Sci*, 50 (2002) 93.
- 37 Dwivedi A K, Kumar Sunil & Tiwari M S, *Astr Space Sci*, 350 (2014) 547.
- 38 Terashima Y, *Prog Theory Phys*, 37 (1967) 775.
- 39 Tiwari M S, Pandey R P & Misra K D, *J Plasma Phys*, 34 (1985) 163.
- 40 Varma P & Tiwari M S, *Phys Scr*, 45 (1992) 275.
- 41 Hasegawa A & Chen L, *Phys Fluids*, 19 (1976) 1924.
- 42 Chen F F, *Introduction to Plasma Physics*, (Plenum Press New York, London), 1974, 34.
- 43 Wygant J R, Keiling A, Cattell C A, Johnson M, Lysak R L, Temerin M, Mozer F S, Kletzing C A, Scudder J D, Peterson W, Russell C T, Parks G, Brittnacher M, Germany G and Spann J, *J Geophys Res*, 105 (2000) 18675.
- 44 Wygant J R, Keiling A, Cattell C A, Lysak R L, Temerin M, Mozer F S, Kletzing C A, Scudder J D, Streltsov V, Lotko W & Russell C T, *J Geophys Res*, 107 (2002) doi: 10.1029/2001JA900113.